Torque Control Accuracy Using Different Techniques for Determination of Induction Motor Rotor Time Constant

# Torque Control Accuracy Using Different Techniques for Determination of Induction Motor Rotor Time Constant

E. Armando, *Senior Member*, IEEE, A. Boglietti, *Fellow*, *IEEE*, F. Mandrile, *Member*, *IEEE*, S. Rubino, *Member*, *IEEE*

***Abstract* – Induction motor (IM) drives represent a competitive solution for both industry and transports electrification. Most control solutions for induction motors currently perform the torque regulation by implementing field-oriented control (FOC) algorithms schemes defined in rotating *dq* coordinates. According to this scenario, the estimation of the *d*-axis position covers a key role to get good accuracy of the torque regulation. If considering the low-speed operation of the motor, the torque control performance is significantly affected by the accuracy in estimating the rotor time constant. According to the literature, this parameter can be computed using either the results of standard- (no-load and locked rotor tests) or flux-decay tests. However, these tests get unequal values of the rotor time constant, thus leading to a different torque control performance. Therefore, this paper aims at investigating the best value of the rotor time constant to optimize the accuracy of the FOC-based torque control. Experimental results obtained on a 4 poles IM, rated 10 kW at 6000 r/min, are presented.**

***Index Terms* -- Field-oriented control, Flux-decay test, Induction machines, Rotor time constant, Standard tests.**

## I. Introduction

THANK their high performance, reliability, and ruggedness, ac motor drives are used in a huge number of industrial applications. The use of induction motors (IMs) in electrical drives represents an economical and reliable solution due to the low cost and the robustness of this machine with respect to other typologies. In the last years, several control typologies have been proposed and adopted to get high performance of adjustable speed drives. According to this scenario, the field-oriented control (FOC) is the most employed torque control algorithm in practice. Indeed, it allows for managing torque and the machine's speed in a straightforward way, getting similar performance to a dc motor drive [1], [2].

In order to perform the torque control, the FOC scheme needs the knowledge of the rotor flux angle [2], [3]. Several FOC techniques are usually implemented in practice according to how this angle is obtained. Anyway, regardless of the considered FOC algorithm (direct-FOC, indirect-FOC, or sensorless methods), the accurate estimation of the rotor time constant is crucial because it is directly connected to the rotor flux controller's performance, i.e., machine torque regulation [4]. Indeed, if the rotor time-constant estimate is wrong, the control performance is derated, as demonstrated in [5]. As a consequence, the correct determination of the rotor time constant is mandatory.

In the literature, there are several solutions for the estimation of the rotor time constant. In [6], the rotor time constant is identified by injecting stator current with an arbitrary frequency. In [7], the measurement method implements a one-phase supply using a dc voltage. In this case, the current value is limited by the stator resistance. Other techniques to estimate the rotor time constant are carried out while the machine is operated in closed-loop speed control, using a dedicated drive scheme. In [8], short rectangular pulses into the flux-producing current reference are applied. In parallel, the torque-producing current reference is analyzed to estimate the rotor time-constant, using the solution of a specific differential time-equation. In [9] and [10], an extended Kalman filter (EKF) is implemented by setting as state variables the stator and rotor currents, together with the reciprocal of the rotor time constant. A model reference adaptive systems (MRAS) is suggested in [11], [12] to produce a model of the IM, thus generating a control error. The MRAS is therefore applied to tune the rotor resistance, providing an accurate convergence. Other techniques apply artificial intelligence (neural networks or fuzzy logic) to estimate the rotor time-constant and so optimally tune the control system [13], [14]. These methods are costly from the computational point of view because they require both estimators and a complex vector space model of the IM, obtained using composite algorithms.

However, despite the existence of the above techniques, the most used method for the determination of rotor time constant is based on the use of the IM parameters obtained from the results of the standard tests like no-load and locked-rotor ones. The no-load test allows the determination of the magnetizing inductance at the rated flux condition, taking into account the magnetic saturation of the machine. In contrast, the locked-rotor test allows the determination of the rotor resistance and leakage inductances. The main drawback of the locked-rotor test is that during the test, the rotor frequency $f_r$ is equal to the stator one $f_s$, while during the normal operating conditions, the rotor frequency depends on the slip $s$ as:

$$f_r = s \cdot f_s \tag{1}$$

The authors are with the Dipartimento Energia "G. Ferraris", Politecnico di Torino, 10129 Turin, Italy (e-mail: eric.armando@polito.it; aldo.boglietti@polito.it; fabio.mandrile@polito.it; sandro.rubino@polito.it).

Since the rated slip of an induction motor is always a few percent, it is well evident that the rotor time constant computed using the locked rotor test parameters is far from the value in the operative conditions. In fact, at the stator frequency, the rotor parameters are affected by the skin effect phenomenon, which alters both the values of the rotor resistance and leakage inductance [15], [16]. In addition, in the presence of closed rotor slots, the rotor leakage inductance is dependent on the magnetic saturation of the slot enclosure, making the value of this parameter non-constant and expressed as a function of the rotor bar current [17].

In [18], a straightforward experimental method is proposed to estimate the IM's rotor time constant based on the flux-decay test. The proposed method allows for determining the rotor time constant at the real operative condition since this test can be performed at the rated voltage and with the rotor speed close to the synchronous one. The machine is initially supplied with a predefined stator voltage level, thus magnetizing the rotor. From a generic moment onwards, the machine supply is suddenly turned off, allowing the measurement of the stator back-emf. Finally, by analyzing the decay of the back-emf, the rotor time constant is evaluated.

According to the above considerations, it is evident how standard- and flux-decay- tests lead to different values of the rotor time constant, which raises the question of the best value to be used for implementing the torque control machine. In this paper, this aspect is investigated by evaluating the accuracy of the torque control using values of rotor time constant obtained with the methods mentioned above. In detail, a FOC-based current vector control (CVC) scheme is used to regulate the torque of a 4 poles IM, rated 10 kW at 6000 r/min.

The paper is organized as follows. Section II briefly summarizes the flux-decay test. Section III describes the CVC scheme used to compare the torque accuracy obtained by each rotor time constant value. Section IV reports the experimental results. Finally, Section V provides paper conclusions.

## II. Flux-Decay Test

In the flux-decay test, the IM under test is initially supplied with the rated stator voltage and frequency and operated in no-load conditions. Then, the stator winding is disconnected from the supply using an electromechanical switch. During the test, the stator voltages are measured, and their evolution is recorded after the supply disconnection. Therefore, the voltage measurements are performed using a data recorder, as reported in the experimental setup shown in Fig. 1.

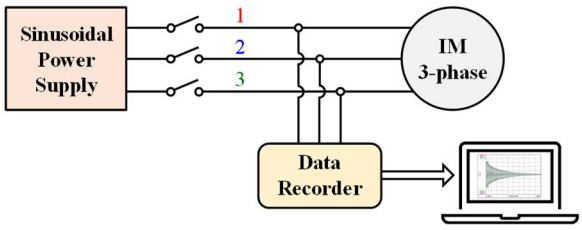


Fig. 1. Experimental setup for performing the flux decay test.

It follows a brief description of the electromagnetic phenomena involved when performing the flux-decay test. According to [18], the IM's voltage model in rotor flux ($dq$) coordinates is the following:

$$\begin{cases} v_{s,d} = R_s \cdot i_{s,d} + \dfrac{d}{dt}\lambda_{s,d} - \omega_s \cdot \lambda_{s,q} \\ v_{s,q} = R_s \cdot i_{s,q} + \dfrac{d}{dt}\lambda_{s,q} + \omega_s \cdot \lambda_{s,d} \\ 0 = R_r \cdot i_{r,d} + \dfrac{d}{dt}\lambda_r \\ 0 = R_r \cdot i_{r,q} + \omega_{slip} \cdot \lambda_r \end{cases} \quad (2)$$

where $(v_{s,d},v_{s,q})$, $(i_{s,d},i_{s,q})$, $(i_{r,d},i_{r,q})$, and $(\lambda_{s,d},\lambda_{s,q})$ are the $(dq)$ components of stator phase voltages, stator phase currents, rotor currents, and stator flux linkages, respectively. The rotor flux amplitude is denoted with $\lambda_r$, while the synchronous speed and electric slip speed are denoted with $\omega_s$ and $\omega_{slip}$, respectively. Finally, $R_s$ and $R_r$ are stator and rotor resistances, respectively. The current model of the machine, consisting of the currents-to-fluxes relationships [18], is the following:

$$\begin{cases} \lambda_{s,d} = L_s \cdot i_{s,d} + L_m \cdot i_{r,d} \\ \lambda_{s,q} = L_s \cdot i_{s,q} + L_m \cdot i_{r,q} \\ \lambda_r = L_m \cdot i_{s,d} + L_r \cdot i_{r,d} \\ 0 = L_m \cdot i_{s,q} + L_r \cdot i_{r,q} \end{cases} \quad (3)$$

where $L_s$, $L_r$, and $L_m$ are the stator-, rotor-, and magnetizing-inductances. According to (2), (3) the following steady-state conditions can be written:

$$\begin{cases} \lambda_r^{ss} = L_m \cdot i_{s,d}^{ss} \\ i_{r,d}^{ss} = 0 \quad , \quad i_{r,q}^{ss} = -\left(L_m / L_r\right) \cdot i_{s,q}^{ss} \\ \lambda_{s,d}^{ss} = L_s \cdot i_{s,d}^{ss} \quad , \quad \lambda_{s,q}^{ss} = \sigma \cdot L_s \cdot i_{s,q}^{ss} \\ v_{s,d}^{ss} = R_s \cdot i_{s,d}^{ss} - \omega_s \cdot \lambda_{s,q}^{ss} \quad , \quad v_{s,q}^{ss} = R_s \cdot i_{s,q}^{ss} + \omega_s \cdot \lambda_{s,d}^{ss} \end{cases} \quad (4)$$

where $\sigma = 1 - L_m^2/(L_s \cdot L_r)$ is the overall leakage factor, while the superscript '$ss$' is used to denote a steady-state quantity before the flux-decay transient happens. It is noted how regardless of the considered load condition, the stator currents practically generate the machine flux.

The flux-decay transient starts when the stator supply is turned off, zeroing the stator currents. It is assumed that the open-circuit event happens quickly, thus considering that stator currents are forced to zero immediately. Therefore, after the open-circuit event, the machine flux is generated by the rotor currents that, in turn, induce back-emf components on the stator voltages. After performing some mathematical manipulations, the back-emf $(e_{s,d},e_{s,q})$ are computed as:

$$\begin{cases} v_{s,d} = e_{s,d} = -\tau_r^{-1} \cdot \left(L_m / L_r\right) \cdot \lambda_r^{ss} \cdot e^{-t/\tau_r} \\ v_{s,q} = e_{s,q} = p \cdot \omega_m \cdot \left(L_m / L_r\right) \cdot \lambda_r^{ss} \cdot e^{-t/\tau_r} \end{cases} \quad (5)$$

where $\omega_m$ is the mechanical speed, $p$ is the pole pair number, while $\tau_r$ is the rotor time constant and whose definition is the following:

$$\tau_r = L_r / R_r \quad (6)$$

According to (5), the back-emf amplitude $e_s$ is computed as:

$$e_s = \sqrt{e_{s,d}^2 + e_{s,q}^2} = \sqrt{\left(p \cdot \omega_m\right)^2 + \left(\tau_r^{-1}\right)^2} \cdot \left(L_m / L_r\right) \cdot \lambda_r^{ss} \cdot e^{-t/\tau_r} \quad (7)$$

By denoting with $\vartheta_r^0$ the initial rotor electric position, after applying the inverse Park transformation $[T_P]^{-1}$ on the machine back-emf ($e_{s,d}$,$e_{s,q}$), the corresponding values in phase coordinates are finally computed as follows:

$$v_{123}^s = e_{123}^s = [T_P]^{-1} \cdot v_{s,dq} = e_s \cdot \begin{bmatrix} \cos\left(p \cdot \omega_m \cdot t + \vartheta_r^0\right) \\ \cos\left(p \cdot \omega_m \cdot t + \vartheta_r^0 - 2\pi/3\right) \\ \cos\left(p \cdot \omega_m \cdot t + \vartheta_r^0 + 2\pi/3\right) \end{bmatrix} \quad (8)$$

According to (8), the time constant associated with the decay of the machine's back-emf corresponds to the rotor time constant since the variations of the rotor speed are negligible while the decay transient happens. However, the following nonlinearities must be considered.

- The magnetizing inductance $L_m$ is not constant due to the saturation phenomena involving both the stator and rotor laminations [15], [16].
- The rotor leakage inductance $L_{lr}$, from which the rotor one depends as $L_r = L_m + L_{lr}$, is subjected to saturation phenomena of the rotor leakage fluxes if the rotor slots are closed [17]. In addition, it is highlighted how also the skin effect affects the value of $L_{lr}$.
- The rotor resistance $R_r$ depends on the rotor temperature and is affected by skin effect [15], [16].

For these reasons, the rotor time constant is not a constant parameter as it depends on the electromagnetic and thermal conditions of the machine. The primary source of variation consists of the skin effect. It is particularly significant when the rotor time constant is computed by measuring the rotor resistance and rotor leakage inductance with a standard locked-rotor test. In this case, the rotor currents have the same frequency as the stator ones, thus maximizing the impact of the skin effect. Therefore, performing the flux-decay test allows getting the following primary advantages.

- The rotor time constant can be measured at the rated flux linkage conditions, thus including the saturation of the jumpers when the rotor slots are of a closed shape.
- The evaluation of the rotor time constant is not affected by the skin effect on the rotor slots as it alters the values of both rotor resistance and rotor leakage inductance.

For the IM used in the experimental validation, the results of the flux-decay test are shown in Fig. 2 and Fig. 3. The machine has been initially supplied in no-load conditions at its rated voltage, i.e., 160 Vrms. After, the stator supply has been suddenly turned off, and the subsequent flux-decay transient of the stator back-emf has been recorded using a data recorder (see Fig. 2). In this way, the envelope of the stator back-emf has been computed as follows:

$$e_s = \sqrt{v_\alpha^{s\,2} + v_\beta^{s\,2}} \quad (9)$$

where the stationary components (αβ) of the stator voltages ($v_\alpha^s$,$v_\beta^s$) have been computed by applying the Clarke transformation $[T_C]$ as:

$$\left[v_\alpha^s \;\; v_\beta^s\right]^t = [T_C] \cdot v_{123}^s \quad (10)$$

Finally, the rotor time constant is obtained by fitting the amplitude of the machine's back-emf using a first-order exponential function.

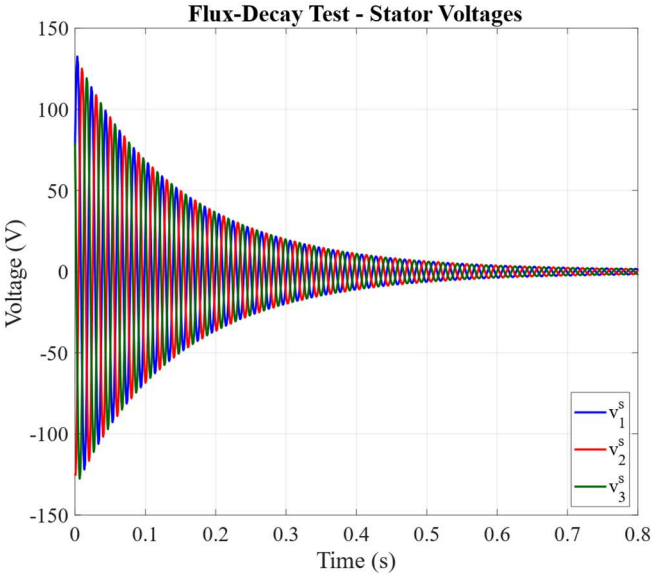


Fig. 2. Measured machine's back-emf during the flux-decay transient.

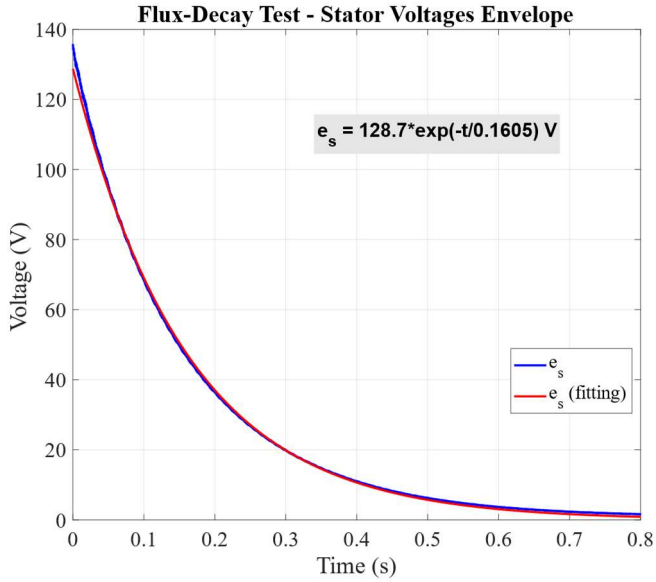


Fig. 3. Measured envelope of the machine's back-emf and fitting profile.

Therefore, measured samples immediately after the stator shut-off directly obtain the initial value of the exponential profile, i.e., 128.7 V. The rotor time constant can be instead computed using a conventional spreadsheet, thus minimizing the sum of the squares of the errors between the fitting profile and the experimental back-emf envelope. The fitting results are shown in Fig. 3, from which the computed value of the rotor time constant corresponds to 160.5 ms.

## III. FOC-BASED CURRENT VECTOR CONTROL SCHEME

To understand the best value of the rotor time constant to get the maximum accuracy of the torque control, a FOC-based CVC has been implemented. According to the literature, two FOC schemes for IM drives can be implemented as follows: direct FOC (D-FOC) and indirect FOC (I-FOC).

The direct field-oriented control (D-FOC) scheme senses the rotor flux vector by using the feedback of electric and mechanical sensors, together with the implementation of dedicated flux observers [2], [3], [19].

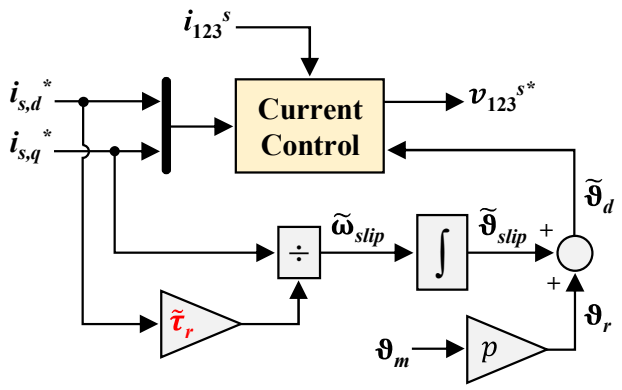


Fig. 4. I-FOC torque control scheme.

Compared to D-FOC, the indirect field-oriented control (I-FOC) indirectly manages the rotor flux orientation, using the feedback of rotor speed and tuning the slip frequency as a function of the stator currents [1]. Although I-FOC does not get the same dynamic performance as D-FOC, it is implemented in most industrial applications that use induction motor drives [20]. However, the rotor flux angle can also be obtained through calculations based on the machine parameters' estimation, using sensorless algorithms [21], [22].

Regardless of the considered FOC algorithm (D-FOC, I-FOC, or sensorless methods), the accurate evaluation of the rotor time constant is crucial because it is directly connected to the estimation of the *d*-axis position, i.e., the rotor flux orientation. Indeed, the torque accuracy is compromised if the rotor time constant estimate is wrong, as demonstrated in [5]. For example, Fig. 4 shows the computation of the rotor flux orientation for the I-FOC scheme. It is noted how the electric slip speed $\omega_{slip}$ is computed from the reference (*dq*) stator currents ($i_{s,d}{}^{*}$,$i_{s,q}{}^{*}$) using the estimated value of the rotor time constant $\tau_r$. If this parameter is not estimated correctly, the rotor flux orientation $\vartheta_d$ is wrong, leading to a steady-state error of the torque regulation. Therefore, through this example, it is pointed out how the proper estimation of the rotor time constant has a significant impact on the torque regulation performance of induction motor drives.

In this paper, the torque control has been implemented using an I-FOC algorithm since it represents the most employed solution in the industry. Referring to Fig. 4, the I-FOC scheme is based on the (*dq*) model of the machine (2), (3). In steady-state conditions, the slip angle $\vartheta_{slip}$ is computed from the stator (*dq*) currents as:

$$\vartheta_{slip} = \int \omega_{slip}\, dt = \int \frac{1}{\tau_r} \cdot \frac{i_{s,q}}{i_{s,d}}\, dt \tag{11}$$

By adding the slip angle to the electric rotor speed $\vartheta_r$ (obtained as pole pair $p$ times that mechanical $\vartheta_m$) the *d*-axis position is thus obtained. Therefore, I-FOC implements (11) using the estimated value of the rotor time constant $\tau_r$ (subscript '^' stands for an estimated variable/parameter) and by considering the stator (*dq*) currents equal to the reference ones. In this way, the need for implementing a rotor flux observer is avoided.

The *d*-axis position is used in the current control to perform the rotational transformations as follows: *i*) obtain the feedback stator (*dq*) currents from those measured in phase coordinates $i_{123}{}^{s}$, and *ii*) compute the reference phase voltages of the machine $v_{123}{}^{s*}$ starting from those defined in (*dq*) coordinates provided by the regulators performing the CVC.

Concerning the reference (*dq*) currents ($i_{s,d}{}^{*}$,$i_{s,q}{}^{*}$), these are computed according to the flux and torque levels. Considering the machine operation below the base speed, the *d*-axis current reference is typically set equal to the rated magnetizing current, thus imposing the rotor flux amplitude to its rated value. Therefore, according to the rated value of magnetizing inductance $L_{m,rated}$ and rotor flux amplitude $\lambda_{r,rated}$, the *d*-axis current reference is computed as follows:

$$i_{s,d}^{*} = \lambda_{r,rated} \big/ L_{m,rated} \tag{12}$$

Finally, the *q*-axis current reference is computed according to the reference torque $T^{*}$. Indeed, starting from (2), (3) the electromagnetic torque of the machine $T_e$ is computed as follows:

$$T_e = \frac{3}{2} \cdot p \cdot \frac{L_m^2}{L_m + L_{lr}} \cdot i_{s,d} \cdot i_{s,q} \tag{13}$$

Therefore, based on (12), (13), the *q*-axis current reference is computed as:

$$i_{s,q}^{*} = \frac{2}{3 \cdot p} \cdot \frac{L_{m,rated} + \tilde{L}_{lr}}{L_{m,rated} \cdot \lambda_{r,rated}} \cdot T^{*} \tag{14}$$

In summary, in the I-FOC scheme, the implemented value of the rotor time constant affects the torque accuracy only in terms of *d*-axis orientation since the reference (*dq*) currents are computed using the currents-to-flux relationships of the machine (i.e., currents-to-torque) [23].

## IV. Experimental Validation

The proposed analysis has been validated on a 4 poles IM (full-pitch windings with four slots/pole/phase), rated 10 kW at 6000 r/min. Table I reports the primary machine data, where the IM parameters have been obtained by performing the no-load and locked-rotor tests at the supply frequency of 50 Hz using a conventional variac. However, the rated frequency of the machine is 200 Hz. Therefore, the locked-rotor test was also performed at the supply frequencies of 100 Hz, 150 Hz, and 200 Hz, obtaining the results summarized in Table II. According to these results, and assuming the magnetizing inductance equal to the rated value $L_m$=$L_{m,rated}$ (see Table I), the rotor time constant is computed using (6). The results are reported in Table III. It is noted how the skin effect leads to a significant increase of the rotor resistance, i.e., as much reduction of the rotor-time constant. Therefore, using the torque controller described in Section III, the best rotor time constant value corresponds to optimizing torque accuracy.

### A. Test rig

The IM under test has been mounted on a test rig for validation purposes. The rotor shaft has been coupled to a driving machine acting as a prime mover, as shown in Fig. 4. To check the accuracy of the torque control scheme, the torque transducer T40B from HBK has been mounted along with the mechanical coupling between IM under test and the driving machine, as shown in Fig. 4.

TABLE I. MACHINE PRIMARY DATA

| Electrical Data | |
|---|---|
| Pole number | 4 |
| Rated power | 10 kW |
| Rated speed | 6000 r/min |
| Rated phase-voltage | 115 Vrms |
| Rated phase current | 10 Arms |
| **Machine Parameters** | |
| Stator resistance $R_s$ | 600 mΩ |
| Leakage inductances $L_{ls}$, $L_{lr}$ @ 50 Hz | 3.96 mH |
| Magnetizing inductance $L_{m,rated}$ | 56.0 mH |
| Rotor resistance $R_r$ @ 50 Hz | 583 mΩ |
| Rated stator flux amplitude $\lambda_{r,rated}$ | 463 mVs |

TABLE II. LOCKED-ROTOR TEST RESULTS

| Frequency (Hz) | $R_r$ (mΩ) | $L_{ls} = L_{lr}$ (mH) |
|---|---|---|
| 50 | 583 | 3.96 |
| 100 | 893 | 3.81 |
| 150 | 1232 | 3.71 |
| 200 | 1575 | 3.63 |

TABLE III. ROTOR TIME CONSTANT FROM STANDARD TESTS

| Frequency (Hz) | $\tau_r$ (ms) |
|---|---|
| 50 | 102.8 |
| 100 | 67.0 |
| 150 | 48.5 |
| 200 | 37.9 |

Fig. 4. View of the IM under test (left), torque transducer (middle), and driving machine (right).

The power converter consists of an IGBT three-phase inverter power module, rated 45 A/1200 V, fed at 540 V by a dc source. Both the switching- and sampling- frequencies have been set at 8 kHz. Finally, the digital controller is the dSPACE® MicroLabBox fast prototyping board, while the control algorithm has been developed in C-code.

## *B. Experimental results*

The experimental results concern the drive operation in torque control mode. The motor speed has been set at 1500 r/min using the driving machine to make the iron losses negligible, and the torque reference has been set at the value of 24 Nm (overload 150 %). The results are shown in Fig. 5 ($T_{meas}$ stands for the measured torque). It is noted how the torque control algorithm is first implemented using the rotor time constant computed from the standard test (ST). Subsequently, the rotor time constant value is suddenly changed to that obtained from the flux-decay test (see flag signal). The torque accuracy is checked using the ST values of rotor time constant for the frequencies reported in Table III, i.e., 50 Hz, 100 Hz, 150 Hz, and 200 Hz.

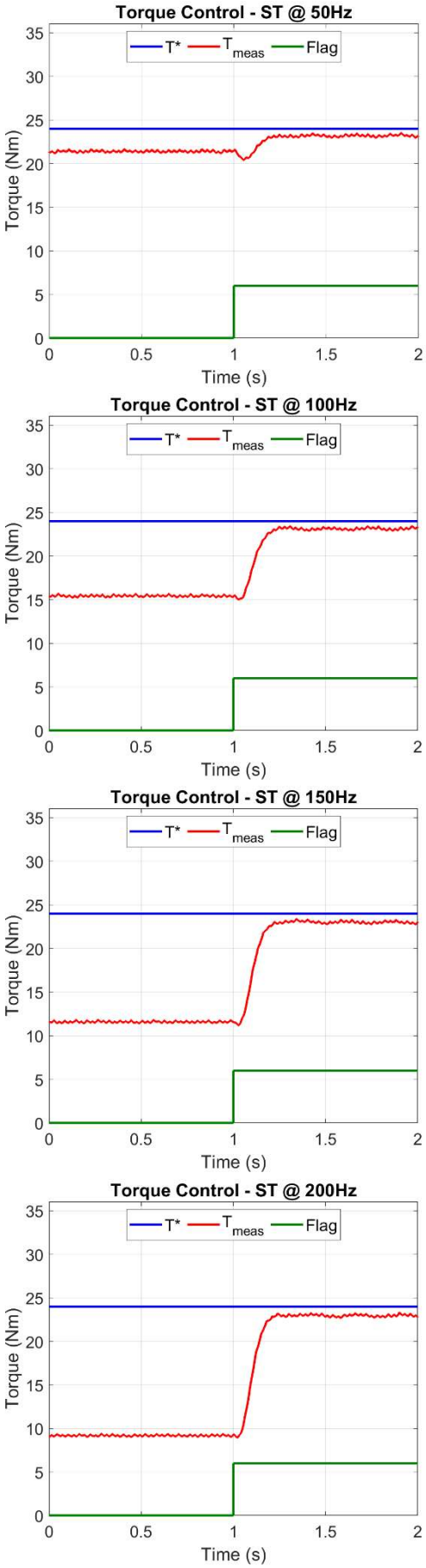


Fig. 5. Torque control accuracy using different rotor time constant values.

TABLE IV. TORQUE ACCURACY RESULTS

| $\tau_r$ Approach | $T^*$ (Nm) | $T_{meas}$ (Nm) | $\Delta T$ (Nm) | $\Delta T$ (%) |
|---|---|---|---|---|
| Flux-Decay | 24 | 23.2 | 0.8 | 3.3 |
| ST @ 50 Hz | 24 | 21.4 | 2.60 | 10.8 |
| ST @ 100 Hz | 24 | 15.6 | 8.4 | 35.0 |
| ST @ 150 Hz | 24 | 11.6 | 12.4 | 51.7 |
| ST @ 200 Hz | 24 | 9.2 | 14.8 | 61.7 |

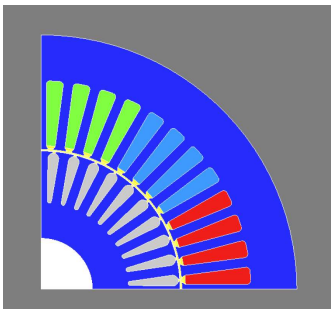

Fig. 6. Layouts of stator and rotor laminations of the IM under test.

It is noted how regardless of the frequency used to tune the rotor time constant values from ST, the value obtained from the flux-decay test leads to higher torque accuracy of the control, as also confirmed in Table IV, which summarizes the obtained results. In detail, the torque accuracy when the rotor time constant is computed from the ST at 200 Hz leads to a significant torque error $\Delta T$ (near 62 %). However, such a frequency is the rated one of the machine, and thus it should be adopted for performing the locked-rotor test [24]. Unfortunately, for inverter-fed IMs like that considered in this paper, the skin effect has a significant impact on the value of rotor resistance due to the shape of the rotor slots, whose layout is shown in Fig. 6.

Therefore, the investigation presented in this paper demonstrates how, for inverter-fed IMs, it is better to obtain the value of the rotor time constant using the flux-decay test instead of combining the results obtained from ST. Indeed, ST are performed at rotor frequencies (hundreds of Hz) much higher than those in regular operation (few Hz). Thus, ST results are affected by the significant errors introduced by the skin effect on the rotor resistance. This issue is all the more evident, the higher the nominal frequency of the motor, as happens for IMs used in traction applications.

## V. CONCLUSION

The paper investigated the best method to compute the rotor time constant of induction motors (IMs) for performing their accurate torque regulation. In detail, two test methods have been considered: *i*) indirect computation of the rotor time constant from standard tests (no-load and locked-rotor ones), and *ii*) direct computation of the rotor time constant from the flux-decay test.

The values of the rotor time constant computed from the above methods have been used to implement a torque control algorithm based on the indirect field-oriented control (I-FOC) scheme, whose *d*-axis orientation is strictly dependent on such a parameter.

Experimental results obtained on 4 poles IM, rated 10 kW at 6000 r/min, have been presented. According to test results, for IMs having a high rated speed/frequency, the rotor time constant obtained from the flux-decay test leads to higher torque control accuracy. Indeed, the flux-decay test is immune to the skin effect phenomena that affect the results of the locked-rotor test, thus leading to the computation of a rotor time constant value near to that encountered in the operative condition of the machine.

## VI. ACKNOWLEDGMENT

The authors would like to acknowledge the financial support from the Power Electronics Innovation Center (PEIC) of Politecnico di Torino (www.peic.polito.it).

## VII. REFERENCES

[1] S.-H. Kim, *Electric Motor Control: DC, AC and BLDC Motors*. Elsevier, 2017.

[2] P. Krause, O. Wasynczuk, S. D. Sudhoff, and S. Pekarek, *Analysis of Electric Machinery and Drive Systems*. John Wiley & Sons, 2013.

[3] A. Amerise, M. Mengoni, L. Zarri, A. Tani, S. Rubino, and R. Bojoi, 'Open-ended induction motor drive with a floating capacitor bridge at variable DC link voltage', in *2017 IEEE Energy Conversion Congress and Exposition (ECCE)*, Oct. 2017, pp. 3591–3597. doi: 10.1109/ECCE.2017.8096638.

[4] T. G. Habetler, F. Profumo, M. Pastorelli, and L. M. Tolbert, 'Direct torque control of induction machines using space vector modulation', *IEEE Trans. Ind. Appl.*, vol. 28, no. 5, pp. 1045–1053, Sep. 1992, doi: 10.1109/28.158828.

[5] S. Chacko, C. Bhende, S. Jain, and R. Nema, 'Modeling and Simulation of Field Oriented Control Induction Motor Drive and Influence of Rotor Resistance Variations on its Performance', *Electr. Electron. Eng. Int. J.*, vol. 5, no. 1, Feb. 2016, doi: 10.14810/elelij.2016.5103.

[6] C. Wang, D. W. Novotny, and T. A. Lipo, 'An automated rotor time-constant measurement system for indirect field-oriented drives', *IEEE Trans. Ind. Appl.*, vol. 24, no. 1, pp. 151–159, Jan. 1988, doi: 10.1109/28.87266.

[7] W. H. Kwon, C. H. Lee, K. S. Youn, and G. H. Cho, 'Measurement of rotor time constant taking into account magnetizing flux in the induction motor', in *Proceedings of 1994 IEEE Industry Applications Society Annual Meeting*, Oct. 1994, vol. 1, pp. 88–92 vol.1. doi: 10.1109/IAS.1994.345494.

[8] S. Wade, W. Dunnigan, and B. W. Williams, 'A new method of rotor resistance estimation for vector-controlled induction machines', *IEEE Trans. Ind. Electron.*, vol. 44, no. 2, pp. 247–257, Apr. 1997, doi: 10.1109/41.564164.

[9] Li-Cheng Zai, C. L. DeMarco, and T. A. Lipo, 'An extended Kalman filter approach to rotor time constant measurement in PWM induction motor drives', *IEEE Trans. Ind. Appl.*, vol. 28, no. 1, pp. 96–104, Jan. 1992, doi: 10.1109/28.120217.

[10] J. Laowanitwattana and S. Uatrongjit, 'Estimation of induction motor states and parameters based on Extended Kalman Filter considering parameter constraints', in *2016 International Symposium on Power Electronics, Electrical Drives, Automation and Motion (SPEEDAM)*, Jun. 2016, pp. 755–760. doi: 10.1109/SPEEDAM.2016.7525829.

[11] A. N. Smith, S. M. Gadoue, and J. W. Finch, 'Improved Rotor Flux Estimation at Low Speeds for Torque MRAS-Based Sensorless Induction Motor Drives', *IEEE Trans. Energy Convers.*, vol. 31, no. 1, pp. 270–282, Mar. 2016, doi: 10.1109/TEC.2015.2480961.

[12] B. Karanayil, M. F. Rahman, and C. Grantham, 'Rotor resistance identification using artificial neural networks for a speed sensorless vector controlled induction motor drive', in *IECON'03. 29th Annual Conference of the IEEE Industrial Electronics Society (IEEE Cat. No.03CH37468)*, Nov. 2003, vol. 1, pp. 419–424 vol.1. doi: 10.1109/IECON.2003.1280017.

[13] E. Bim, 'Fuzzy optimization for rotor constant identification of an indirect FOC induction motor drive', *IEEE Trans. Ind. Electron.*, vol. 48, no. 6, pp. 1293–1295, Dec. 2001, doi: 10.1109/41.969416.

[14] S. Yang, D. Ding, X. Li, Z. Xie, X. Zhang, and L. Chang, 'A Novel Online Parameter Estimation Method for Indirect Field Oriented

Induction Motor Drives', *IEEE Trans. Energy Convers.*, vol. 32, no. 4, pp. 1562–1573, Dec. 2017, doi: 10.1109/TEC.2017.2699681.
[15] A. Boglietti, A. Cavagnino, and M. Lazzari, 'Computational Algorithms for Induction-Motor Equivalent Circuit Parameter Determination—Part I: Resistances and Leakage Reactances', *IEEE Trans. Ind. Electron.*, vol. 58, no. 9, pp. 3723–3733, Sep. 2011, doi: 10.1109/TIE.2010.2084974.
[16] A. Boglietti, A. Cavagnino, and M. Lazzari, 'Computational Algorithms for Induction Motor Equivalent Circuit Parameter Determination—Part II: Skin Effect and Magnetizing Characteristics', *IEEE Trans. Ind. Electron.*, vol. 58, no. 9, pp. 3734–3740, Sep. 2011, doi: 10.1109/TIE.2010.2084975.
[17] A. Boglietti, R. I. Bojoi, A. Cavagnino, P. Guglielmi, and A. Miotto, 'Analysis and Modeling of Rotor Slot Enclosure Effects in High-Speed Induction Motors', *IEEE Trans. Ind. Appl.*, vol. 48, no. 4, pp. 1279–1287, Jul. 2012, doi: 10.1109/TIA.2012.2199270.
[18] E. Armando, A. Boglietti, S. Musumeci, and S. Rubino, 'Flux-Decay Test: A Viable Solution to Evaluate the Induction Motor Rotor Time-Constant', *IEEE Trans. Ind. Appl.*, vol. 57, no. 4, pp. 3619–3631, Jul. 2021, doi: 10.1109/TIA.2021.3076425.
[19] S. Rubino, R. Bojoi, F. Mandrile, and E. Armando, 'Modular Stator Flux and Torque Control of Multiphase Induction Motor Drives', in *2019 IEEE International Electric Machines Drives Conference (IEMDC)*, San Diego, USA, May 2019, pp. 531–538. doi: 10.1109/IEMDC.2019.8785376.
[20] I. Ferdiansyah, M. R. Rusli, B. Praharsena, H. Toar, Ridwan, and E. Purwanto, 'Speed Control of Three Phase Induction Motor Using Indirect Field Oriented Control Based on Real-Time Control System', in *2018 10th International Conference on Information Technology and Electrical Engineering (ICITEE)*, Jul. 2018, pp. 438–442. doi: 10.1109/ICITEED.2018.8534864.
[21] C. C. de Azevedo, C. B. Jacobina, L. A. S. Ribeiro, A. M. N. Lima, and A. C. Oliveira, 'Indirect field orientation for induction motors without speed sensor', in *APEC. Seventeenth Annual IEEE Applied Power Electronics Conference and Exposition (Cat. No.02CH37335)*, Mar. 2002, vol. 2, pp. 809–814 vol.2. doi: 10.1109/APEC.2002.989337.
[22] D. Xu, B. Wang, G. Zhang, G. Wang, and Y. Yu, 'A review of sensorless control methods for AC motor drives', *CES Trans. Electr. Mach. Syst.*, vol. 2, no. 1, pp. 104–115, Mar. 2018, doi: 10.23919/TEMS.2018.8326456.
[23] O. Stiscia, S. Rubino, S. Vaschetto, A. Cavagnino, and A. Tenconi, 'Accurate Induction Machines Efficiency Mapping Computed by Standard Test Parameters', *IEEE Trans. Ind. Appl.*, pp. 1–1, 2022, doi: 10.1109/TIA.2022.3156921.
[24] '112-2017 - IEEE Standard Test Procedure for Polyphase Induction Motors and Generators'. https://ieeexplore.ieee.org (accessed Apr. 09, 2021).

## VIII. BIOGRAPHIES

**Eric Armando** (Senior Member, IEEE) received the M.Sc. and Ph.D. degrees in electrical engineering from Politecnico di Torino, Turin, Italy, in 2002 and 2008, respectively.,He is currently an Associate Professor of power converters, electrical machines and drives with Politecnico di Torino. His research interests include power electronics and high performance ac motor drives. He is the coauthor of numerous journal papers and of three patents.,Dr. Armando was the recipient of three awards for innovation and one paper award from the Power Electronics Technical Committee of the IEEE Industrial Electronics Society.

**Aldo Boglietti** (Fellow, IEEE) was born in Rome, Italy. He received the Laurea degree in electrical engineering from the Politecnico di Torino, Torino, Italy, in 1981. He started his research work with the Department of Electrical Engineering, Politecnico di Torino as a Researcher of Electrical Machines in 1984. He was an Associate Professor of Electrical Machines in 1992, and has been a Full Professor with the same University, since 2000. He was the Head of the Electrical Engineering Department, Politecnico of Torino, from 2003 to 2011. Prof. Boglietti was the Chair of the Electrical Machines Committee of the IEEE Industry Applications Society and the Chair of the Electrical Machines Technical Committee of the IEEE Industrial Electronics Society. He is a Reviewer for many IEEE transactions and other international journals.

**Fabio Mandrile** (S'18, M'21) received the M.Sc. and Ph.D. degrees in electrical engineering in 2017 and 2021, respectively, from Politecnico di Torino, Torino, Italy. His main research interests include virtual synchronous generators, power electronics for grid-connected applications and the experimental characterization of converters and motor drives.

**Sandro Rubino** (Member, IEEE) received the M.Sc. and Ph.D. degrees in electrical engineering from the Politecnico di Torino, Torino, Italy, in 2014 and 2019, respectively. He is currently an Assistant Professor with the Dipartimento Energia "G. Ferraris," Politecnico di Torino. His main research interests include power electronics, modeling, and control of multiphase electrical machines and high-performance ac motor drives. Dr. Rubino was a recipient of One Paper Award from the Industrial Drives Committee of the IEEE Industry Applications Society and two Ph.D. Thesis Awards from the IEEE Power & Energy Society Italy Chapter and IEEE Industrial Electronics Society Italy Chapter. He serves as a Reviewer for some IEEE transactions and international conferences.